Available online at www.sciencedirect.com

ScienceDirect

Energy Procedia 77 (2015) 791 – 798

Energy Procedia

5th International Conference on Silicon Photovoltaics, SiliconPV 2015

Morphology and hydrogen in passivating amorphous silicon layers

Sebastian Gerke[a,*], Hans-Werner Becker[b], Detlef Rogalla[b], Giso Hahn[a], Reinhart Job[c], Barbara Terheiden[a]

[a]*University of Konstanz, Department of Physics, Konstanz, 78457, Germany*
[b]*RUBION - Central Unit for Ion Beams and Radioisotopes, University of Bochum, Universitätsstraße 150, Bochum, 44780, Germany*
[c]*Department of Electrical Engineering and Computer Science, Münster University of Applied Sciences, Stegerwaldstraße 39, Steinfurt, 48565, Germany*

Abstract

Hydrogenated intrinsic amorphous silicon ((i) a-Si:H) can be grown by plasma-enhanced chemical vapor deposition with a non-columnar or columnar morphology. Nuclear resonant reaction analysis and corresponding effective stopping cross section analysis indicate a dependency of hydrogen effusion on the morphology of the (i) a-Si:H layer as well as the doping type and concentration of the c-Si wafer. The doping type of the c-Si wafer also affects the growth of the amorphous network. It is found that for moderately doped p-type c-Si a non-columnar (i) a-Si:H layer yields a significantly better and more stable passivation already during thermal anneal and illumination, while for passivating n-type c-Si a columnar layer is recommended. Passivating lowly doped c-Si by (i) a-Si:H is not dependent on morphology. Combining different (i) a-Si:H morphologies to a multi-layer stack improves the quality of surface passivation. Hydrogen embedded in a well passivating but hydrogen-permeable columnar layer supports good surface passivation when covered by a non-columnar layer, featuring a fast growing layer acting as a hydrogen barrier and enhancing surface passivation quality.

Peer review by the scientific conference committee of SiliconPV 2015 under responsibility of PSE AG

Keywords: a-Si; passivation; FTIR; NRRA; hydrogen depth profiling; multi-layer stack; stability; annealing

* Corresponding author. Tel.: +49-7531-88-2132; fax: +49-7531-88-3895.
E-mail address: sebastian.gerke@uni-konstanz.de

Peer review by the scientific conference committee of SiliconPV 2015 under responsibility of PSE AG
doi:10.1016/j.egypro.2015.07.112

1. Introduction

Plasma-enhanced chemical vapour deposition (PECVD) of (i) a-Si:H on c-Si provides excellent surface passivation [1, 2, 3]. The silane/argon (SiH_4/Ar) ratio during deposition leads to columnar or non-columnar growth of the (i) a-Si:H layer [1, 2, 4-6]. For the non-columnar structure a fast growing layer (FGL) during early deposition was reported [2, 7, 8]. Nuclear resonant reaction analysis (NRRA) has shown that changes in hydrogen distribution during thermal treatment are related to the (i) a-Si:H morphology [2]. An enhanced effusion of hydrogen out of a columnar layer compared to a non-columnar one was observed [2].

Up to now, there exists no detailed analysis of differently doped c-Si surfaces passivated by (i) a-Si:H layers of varying morphologies. Furthermore, the application of a non-columnar layer providing a fast growing layer (FGL) as hydrogen effusion barrier on top of a columnar layer enhancing passivation quality has not yet been investigated.

2. Sample preparation and experimental conditions

The here investigated (i) a-Si:H layers are PECV-deposited using a PlasmaLab 100 direct plasma reactor from Oxford Instruments. While an (i) a-Si:H deposition using only silane results in a non-columnar morphology of the layer, a SiH_4/Ar mixture yields a columnar growth of the amorphous network. More information and details on deposition parameters are given in [2]. For the experiments phosphorous as well as boron doped chemically polished float-zone (FZ) silicon wafers (c-Si) are used (n-type: 1 Ωcm (500 µm); 5 Ωcm and 200 Ωcm (250 µm); p-type: 1 Ωcm and 200 Ωcm (250 µm); all wafers <100> oriented). Native oxide at the surface of the c-Si wafers is chemically removed in diluted hydrogen fluoride (HF) directly before PECV-deposition [2]. Several (i) a-Si:H layers of different morphology are prepared by PECVD (single layers as well as multi-layer stacks). Multi-layer stacks provide a columnar layer at the (i) a-Si-H/c-Si interface which is covered by a non-columnar layer.

As there exists no method for a direct investigation of the morphology of an (i) a-Si:H layer, the morphology is studied by indirect methods like scanning electron microscopy (SEM) investigations of thick (i) a-Si:H (> 5 µm) deposited over trenches using a Zeiss Neon 40 SEM [9]. As mentioned in [2] the Si-H_x bonding structure of an (i) a-Si:H layer also allows to draw conclusions on the morphology of the amorphous layer. Such investigations are carried out by Fourier transformed infrared (FTIR) spectroscopy using a Bruker Vertex 80 spectrometer [2].

The passivation of the (i) a-Si:H layers is activated during 4 min of thermal treatment on a hotplate in ambient air. The non-columnar layers are activated at 300°C [7] and the columnar ones at 200°C [4].

Samples were afterwards further annealed in ambient air and on a hotplate at 200°C in the dark (morphology independent) [2, 4] or illuminated by a halogen lamp in ambient air at an illumination level of 1 sun (100 mW/cm²) at 50°C [10]. Changes in the effective stopping cross section (scs_{eff}) of the (i) a-Si:H are investigated by nuclear resonant reaction analysis (NRRA) [11-14].

In addition, the evolution of the passivation quality is investigated by changes in the effective minority carrier lifetime (τ_{eff}) measured by quasi steady state photoconductance using a WCT 120 from Sinton Instruments [1-4, 15]. To compare the passivation quality of differently doped samples, the τ_{eff} related surface recombination velocity (SRV: S_{eff}) is calculated and compared during thermal treatment as well as illumination [3, 7, 16].

3. Morphology of amorphous silicon

The morphology of an (i) a-Si layer can be influenced by the deposition parameters. Depositing pure silane (SiH_4) leads to a non-columnar, random growth of the amorphous network. Supplementary argon yields a columnar, chain-like growth by increasing the sticking factor of the process gas mixture [1, 2, 4 ,6].

Vacancies arising during deposition mainly affect the quality of (i) a-Si:H films by supporting dangling bonds. According to Ref. [2, 4 ,6] the type of vacancy also depends on the morphology of the a-Si layer. An amorphous non-columnar network contains mainly single voids. In contrast, a columnar growth of the a-Si layer supports the formation of aligned vacancies, so called microvoids [6] (Fig. 1, b and c).

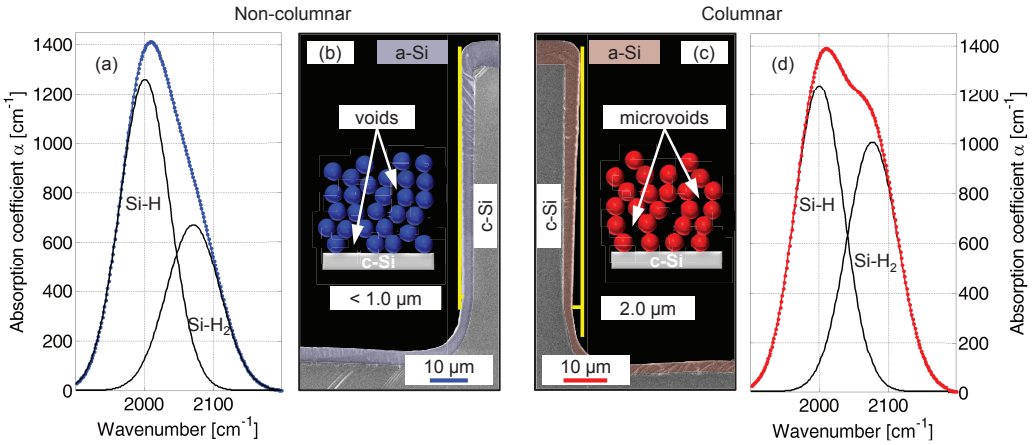

Fig. 1. Illustrations of the non-columnar (b) and columnar a-Si structure (c) and specific vacancies as well as SEM investigations of (i) a-Si:H layers PECV-deposited in trenches of the substrate visualizing morphological differences. (a and d) FTIR-spectroscopical analyses of the Si-H_x bonding structure of a non-columnar (a) and a columnar (d) layer. (a-b): Properties of a non-columnar (i) a-Si:H layer; (a): low Si-H_2 content, (b): high surface conformity. (c-d): Properties of a columnar (i) a-Si:H layer; (c): low surface conformity, (d): high Si-H_2 content.

Because of the amorphous structure, it is not easy to use the contrast of high resolution transmission electron microscopes to investigate such sub-nanoscopic structures. Therefore, indirect methods have to be used to classify the morphology of an a-Si layer. One indicator is the Si-H_2 bond structure [2, 6]. In Fig. 1 (a) and (d) FTIR spectra of a non-columnar (a) and a columnar (d) PECV-deposited (i) a-Si:H layer are shown. A low Si-H_2 content indicates non-columnar a-Si:H (Fig. 1, a), whereas a comparatively high Si-H_2 content is linked to columnar a-Si:H (Fig. 1, d).

Analysis of (i) a-Si:H covering trenches in the substrate provides additional information. Due to Ar included while depositing a columnar a-Si:H layer, the surface mobility of Si atoms decreases and atoms attach faster to the growing layer at their final positions [1]. This leads to a higher growth rate but also to a lower surface conformity of a columnar layer compared to a non-columnar one [2]. Fig. 1 (b) and (c) show such trench analyses of a non-columnar (b) and a columnar (i) a-Si:H layer (c) covering 80 µm wide and deep trenches in a c-Si surface. The aforementioned differences in surface conformity are shown in the SEM images. While the non-columnar (i) a-Si:H layer deviates < 1 µm from the vertical (yellow line in Fig. 1, b), the deviation from the vertical of the columnar layer is ~2.0 µm (Fig. 1, c).

Further investigations of non-columnar (i) a-Si:H layers deposited using the same setup and parameters as in this study have shown that a so called fast growing layer (FGL) forms at the (i) a-Si:H/c-Si interface [7, 8]. Analysis of hydrogen depth profiles measured by NRRA before and after thermal treatment (100 h at 200°C) indicates that there is hardly any effusion of hydrogen out of the FGL and only little effusion out of the non-columnar layer itself (~0.3%) [2]. Comparative NRRA investigations have indicated that the hydrogen effusion out of a columnar (i) a-Si:H layer is higher at ~0.9%.

4. Nuclear resonant reaction analysis

NRRA [2, 11-14] not only provides information about the hydrogen distribution in a layer, but is also able to determine the effective stopping cross section (scs_{eff}) [14]. scs_{eff} permits direct comparison of samples with unknown hydrogen content in a known standard (so called *matrix*). This density-independent method is well suited to investigate (i) a-Si:H of different morphologies. scs_{eff} (eq. 1) is calculated by weighing the measured hydrogen content (N_H) with scs of hydrogen ($scs_H = 60.9 \cdot 10^{-15}$ eV/(at./cm²)) and compare it with the scs of the matrix (i.e. c-Si) ($scs_M = 279 \cdot 10^{-15}$ eV/(at./cm²)) [17]. Assuming hydrogen and the matrix are the only atoms in the layer, N_M can be calculated as $N_M = 1\text{-}(N_{MSi}/N_H)$ with the atomic density of silicon $N_{MSi} \approx 5 \cdot 10^{22}$ at./cm³ [14, 18].

$$scs_{eff} = N_H \cdot scs_H + N_M \cdot scs_M \quad (1)$$

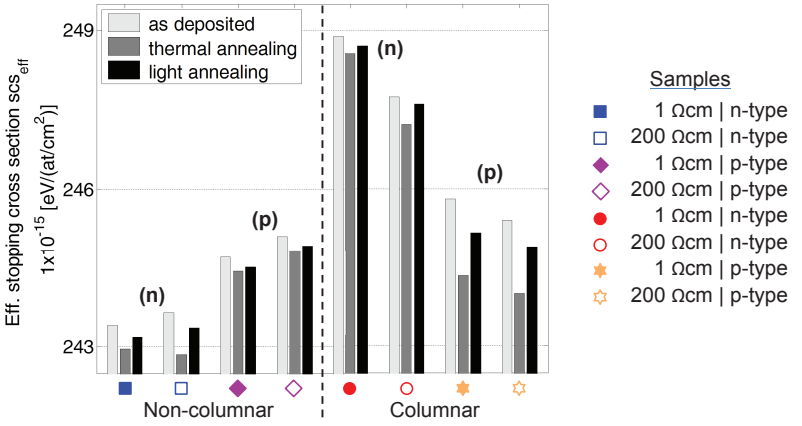

Fig. 2. 40 nm thin (i) a-Si:H layers PECV-deposited to different morphologies on 1 Ωcm and 200 Ωcm n- and p-type c-Si and NRR-analyzed. Displayed are the calculated effective stopping cross sections (scs_{eff}) of as-deposited, thermally annealed and illuminated samples.

For comparison, scs_{eff} of the German national (i) a-Si:H standard with a hydrogen content of ~12% is $scs_{eff} = 252 \cdot 10^{-15}$ eV/(at./cm²) as given in [19].

While layers lose hydrogen during thermal treatment [1, 2], it can be assumed that the amount of Si atoms remains constant. Therefore, N_M is kept constant at the value of the as deposited state for determination of scs_{eff} of annealed samples.

Fig. 2 shows scs_{eff} for 40 nm thin as deposited and not activated, activated and thermally annealed (100 h) and activated and illuminated (21 d) samples of different morphologies deposited on differently doped c-Si (1 Ωcm and 200 Ωcm, n- and p-type). Filled marks represent 1 Ωcm c-Si samples and unfilled marks represent 200 Ωcm c-Si samples. (■, □, ◆, ◇) represent non-columnar (i) a-Si:H layers, while (●, ○, ✸, ✡) represent columnar (i) a-Si:H layers.

As can be seen in Fig. 1 (a), scs_{eff} of all layers is lower than scs_M of pure c-Si and slightly lower than the mentioned German national (i) a-Si:H standard [19]. Non-columnar (i) a-Si:H layers (■, □, ◆, ◇) show lower scs_{eff} values compared to columnar layers (●, ○, ✸, ✡) especially for as deposited (▭) samples. In more detail, the scs_{eff} values of non-columnar (i) a-Si:H layers deposited on n-type (■, □) are slightly lower than for p-type c-Si (◆, ◇), $\Delta_{(scseff)} \approx 1 \cdot 10^{-15}$ eV/(at./cm²). The obvious high difference in scs_{eff} of $\Delta_{(scseff)} \approx 3 \cdot 10^{-15}$ eV/(at./cm²) between the columnar (i) a-Si:H layers deposited on n-type c-Si (●, ○) and those layers deposited on p-type c-Si (✸, ✡) indicates a different growth mechanism of the amorphous network. These structural differences might be more distinctive in the columnar (i) a-Si:H layers compared to the non-columnar ones.

In addition, scs_{eff} of columnar layers deposited on p-type c-Si (✸, ✡) show a larger decrease in scs_{eff} during thermal annealing (▬) than those deposited on n-type c-Si (●, ○). This might be due to a faster diffusion of hydrogen in moderately doped p-type FZ c-Si compared to moderately doped n-type FZ c-Si [1, 6, 20].

In case of illumination (■), scs_{eff} decreases far less compared to thermal annealing. But the previously described trends of the scs_{eff} values during thermal treatment persist during illumination.

5. Morphology dependent passivation

Investigating scs_{eff} leads to the hypothesis that passivation qualitiy of (i) a-Si:H layers depends on layer morphology as well as doping type and doping level of the c-Si wafer.

Gerke *et al*. have shown that the passivation quality of a non-columnar (i) a-Si:H layer deposited on 5 Ωcm n-type c-Si remains stable during thermal treatment at 200°C [2]. It was further shown that the passivation quality of a columnar (i) a-Si:H layer also deposited on 5 Ωcm n-type c-Si decreases during analogous thermal treatment [2, 4]. This significant difference is related to the above mentioned fast growing layer at the (i) a-Si:H/c-Si interface of a non-columnar layer, as the FGL prevents hydrogen effusion whereby the stability of the passivation quality increases [2, 7].

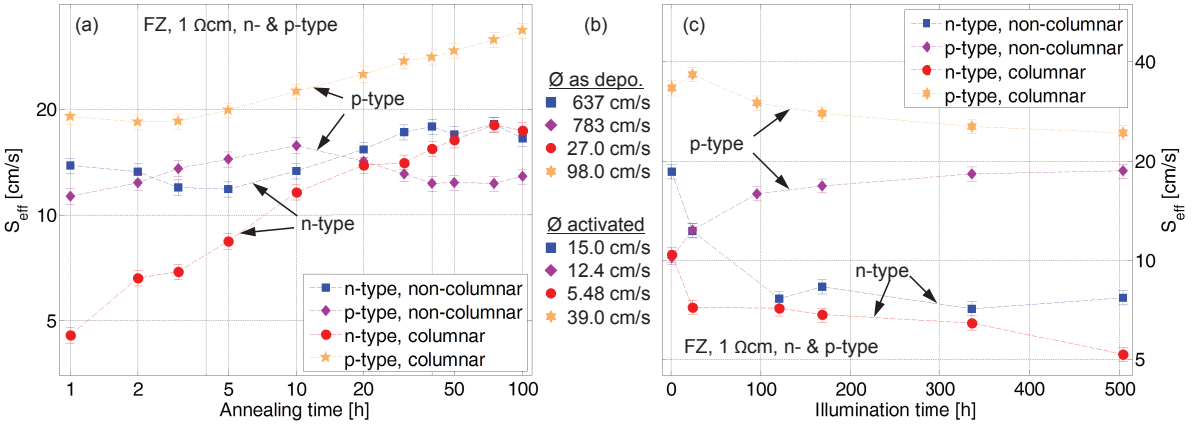

Fig. 3. 40 nm thin (i) a-Si:H layers PECV-deposited to different morphologies on 1 Ωcm n- and p-type c-Si. Evolution of S_{eff} during thermal annealing (a) of 100 h at 200°C, and illumination (c) for 3 weeks at 1 sun and 50°C. Lines are guides to the eye. (b): S_{eff} values determined after deposition and after thermal activation prior to thermal annealing or illumination.

5.1. Passivating moderately doped c-Si

Fig. 3 (a) shows the evolution of S_{eff} comparing non-columnar and columnar (i) a-Si:H layers deposited on 1 Ωcm n- and p-type c-Si during 100 h of thermal treatment at 200°C. All (i) a-Si:H layers confirm the previously mentioned published trends regardless of the kind of c-Si doping type.

Fig. 3 (b) and (c) show the behavior of S_{eff} during illumination up to 504 h (3 weeks) (c) and the values of S_{eff} directly after deposition and after a 4 min thermal activation step (b). As can be seen in Fig. 3 (b), passivation quality of all layers increases during the activation step. The evolution of S_{eff} during thermal treatment (Fig. 3, a) shows that S_{eff} for c-Si passivated with columnar (i) a-Si:H (●,✸) decreases between activation and the first hour of annealing.

Starting at one hour of thermal treatment S_{eff}, of the columnar (i) a-Si:H samples differ significantly by about 15 cm/s ●,✸ during annealing. In more detail, while S_{eff} of the n-type sample ● increases from 4 to 18 cm/s, S_{eff} of the p-type sample ✸ increases from 19 to 33 cm/s. In contrast, the non-columnar layers ■,◆ passivate p- as well as n-type c-Si on the same level of 10 to 15 cm/s and passivation quality remains stable after the activation step over the whole range of annealing durations.

Effects like photo-induced curing [21] and different mobility of charged hydrogen [1, 20-22] may make S_{eff} in case of illuminated annealing of activated (i) a-Si:H samples dependent on the c-Si doping type, Fig. 3 (c). S_{eff} of n-type c-Si ■, ● shows values independent of (i) a-Si:H morphology. In contrast, S_{eff} of p-type c-Si ✸,◆ varies much more. During illumination S_{eff} of ✸ (p-type c-Si, passivated with columnar (i) a-Si:H) saturates on a stable level at 24 cm/s. The reason for the strong increase in S_{eff} for the p-type c-Si with non-columnar layers ◆ from 12 to 19 cm/s might be a Staebler-Wronski-like degradation [1, 23, 24]. But such degradation cannot be determined for any other sample type. However, it cannot be excluded that degradation occurs for longer annealing [10] or higher illumination densities [25].

5.2. Passivating lowly doped c-Si

Additional evaluations of S_{eff} of non-columnar and columnar (i) a-Si:H layers PECV-deposited on 200 Ωcm n- and p-type c-Si are given in Fig. 4. Comparing the evolution of S_{eff} during thermal treatment of 1 Ωcm (Fig. 3, a) and 200 Ωcm (Fig. 4, a), the behavior of S_{eff} is partial quite different. Starting with the similarities it can be seen in Fig. 3 as well as in Fig. 4 that after the activation step S_{eff} of the columnar (i) a-Si:H samples first decreases, but increases during thermal treatment. This further improvement of passivation quality of the columnar (i) a-Si:H layers after the activation step of columnar (i) a-Si:H layers deposited on 1 Ωcm and 200 Ωcm is different to layers deposited on 5 Ωcm, see section 6 and Ref. [8].

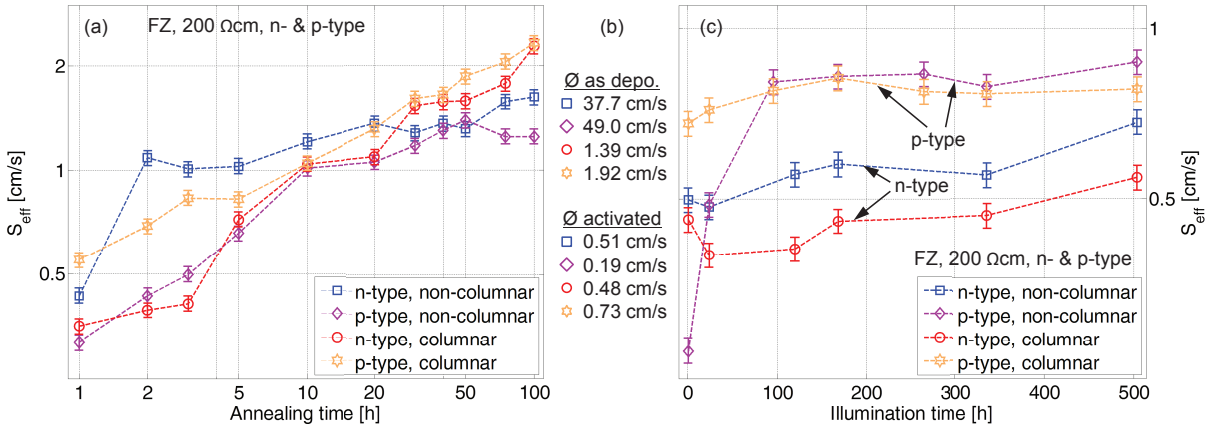

Fig. 4. 40 nm thin (i) a-Si:H layers PECV-deposited to different morphologies on 200 Ωcm n- and p-type c-Si. Evolution of S_{eff} during thermal annealing (a) of 100 h at 200°C, and illumination (c) for 3 weeks at 1 sun and 50°C. Lines are guides to the eye. (b): S_{eff} values determined after deposition and after thermal activation.

As can be seen in Fig. 4 (a), S_{eff} of all layers increases continuously during the observed duration of thermal treatment of 100 h regardless of the kind of c-Si doping type. This behavior differs from the observed trends of S_{eff} of 1 Ωcm samples during annealing discussed in section 5.1 (Fig. 3, a).

In contrast, the evolution of S_{eff} during illumination (Fig. 4, c) is similar to the evolution of the observed 1 Ωcm samples (Fig. 3, c). There is a clear distinction between S_{eff} of p-type samples (◇,☆) and n-type samples (□,○). With focus on the p-type samples ◇,☆ the non-columnar (i) a-Si sample (◇) is outstanding. After activation (S_{eff} = 0.19 cm/s) S_{eff} increases rapidly during 96 h (4 d) of illumination to $Seff$ = 0.8 cm/s. During further illumination, S_{eff} of p-type c-Si ◇,☆ show stable and (i) a-Si:H morphology-independent values. S_{eff} of n-type c-Si □,○ is nearly identical after activation. S_{eff} of both (i) a-Si:H layers slightly increases during illumination, while the columnar layer ○ decreases at first before showing a stable offset of ~0.1 cm/s to □.

Apart from the non-columnar (i) a-Si:H, p-type c-Si sample (◇), a Staebler-Wronski-like degradation cannot be determined for the illuminated 200 Ωcm samples. This correlates to the previously discussed evolution of 1 Ωcm c-Si samples (Fig. 3, a).

6. Multi-layer stack

Combining the benefits of a non-columnar layer including a FGL and a columnar one, layer stacks of a non-columnar on top of a columnar (i) a-Si:H layer are prepared, see Fig. 5 (c). The passivated 5 Ωcm, n-type c-Si undergoes the same activation as used for the columnar single layer and thermal treatment as well as illumination as described in section 2, because the (i) a-Si:H at the (i) a-Si:H/c-Si interface of the stack is also columnar (Fig. 5, c).

6.1. Hydrogen distribution

Fig. 5 (a) shows the changes in hydrogen distribution measured by NRRA [2, 11-13] of an (i) a-Si:H multi-layer stack of 100 nm total thickness before (●) and after (■) thermal annealing (100 h at 200°C).

Loss in hydrogen near the (i) a-Si:H/c-Si interface as well as near the surface is observable, as is the functionality of a FGL as hydrogen barrier or drain layer. As can be seen, hydrogen diffused away from the (i) a-Si/c-Si interface to accumulate in the FGL as hydrogen from the non-columnar layer does (Fig. 5, a). It can be estimated that the non-columnar (i) a-Si:H layer mainly loses hydrogen to the ambient at the sample surface, whereas hydrogen effusing from the columnar layer accumulates in the FGL or rather in front of it. In absolute numbers, only <0.5%$_{abs}$ of hydrogen effuses out of the multi-layer stack during thermal treatment compared to ~1%$_{abs}$ for a columnar single layer [2]. With respect to the hydrogen depth profile measured after thermal treatment (■), the maximum hydrogen content of the FGL saturates at 19.4%.

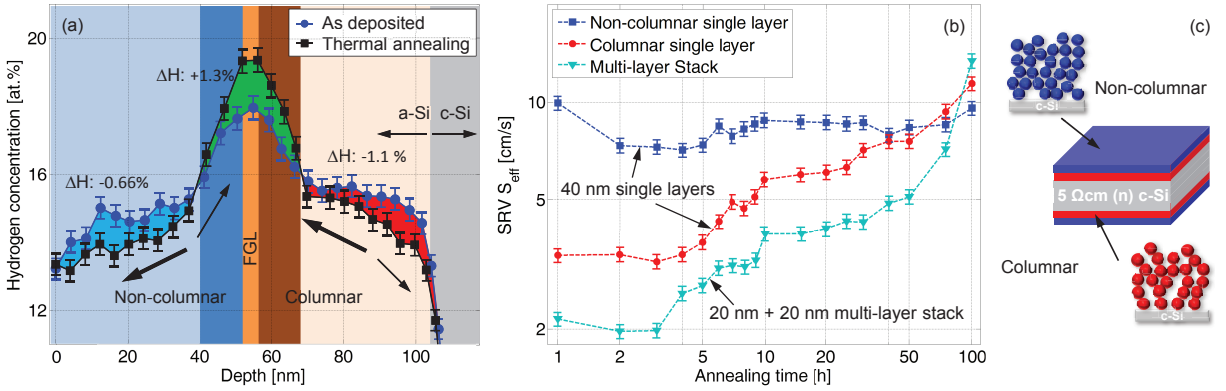

Fig. 5. (a): NRRA hydrogen concentration profiles of a 100 nm PECV-deposited (i) a-Si:H multi-layer stack of different morphologies measured directly after deposition and after thermal annealing. (b): Evolution of S_{eff} of 40 nm thin non-columnar and columnar single layers compared to a 40 nm thin multi-layer stack during thermal. Lines are guides to the eye. (c): Schematic of the multi-layer stack.

6.2. Passivation quality

S_{eff} values of all samples are equal within measurement accuracy after the activation step to those after 1 h of thermal treatment shown in Fig. 5 (b). The investigated 40 nm non-columnar single layer (■) passivates the 5 Ωcm c-Si as mentioned in section 5 for medium doped c-Si and passivation quality remains stable during thermal treatment (Fig. 5, b). S_{eff} of a 40 nm multi-layer stack (▼) develops like a comparable columnar single layer (●) and increases during thermal treatment. The stack system provides a higher passivation quality of S_{eff}, for the first ~90 h of thermal treatment.

In more detail, S_{eff} of the columnar (i) a-Si:H layer (●) remains stable at ~3.4 cm/s during the first 4 h of thermal treatment before increasing to S_{eff} = 11.4 cm/s after 100 h. In comparison, S_{eff} of the multi-layer stack (▼) remains stable at a lower level of ~2 cm/s during the first 3 h of thermal treatment. As can be seen in Fig. 5 (b) there are three step-like increases of S_{eff} between 3-4 h, 5-6 h and 9-10 h before S_{eff} remains relatively stable at ~4 cm/s until 30 h of thermal treatment. Between 30-50 h S_{eff} of the multi-layer stack ▼ lightly increases to 5 cm/s before passivation quality decreases rapidly to 13.4 cm within the next 50 h.

Moreover, illumination does not show any further influence compared to the investigations discussed in section 5, neither to the single layers nor to the multi-layer stack (not shown). S_{eff} of a multi-layer stack behaves as S_{eff} of a columnar single layer during illumination and remains stable on the respective activation level.

7. Conclusions

Hydrogen content and scs_{eff} as well as passivation quality of PECV-deposited (i) a-Si:H layers are influenced by the layer morphology and the c-Si base doping. The c-Si base doping also affects the growth of the respective (i) a-Si:H network and hereby the passivation quality of the layer. For passivation of p-type c-Si a non-columnar layer and for passivation of n-type c-Si a columnar layer can be recommended. Due to less hydrogen effusion, passivation using an (i) a-Si:H multi-layer stack composed of a first columnar and second non-columnar layer offers higher passivation quality comparable to a columnar single layer. The columnar layer at the (i) a-Si:H/c-Si interface supports good surface passivation while being covered by a non-columnar layer, featuring a fast growing layer which acts as hydrogen barrier layer.

Acknowledgements

Part of this work was supported by the German Federal Ministry for the Environment, Nature Conservation and Nuclear Safety (FKZ 0325581). The content is the responsibility of the authors.

The authors would also like to thank E. Emre for supporting this paper and A. Frey for grinding the trenches. Special thanks go to the RUBION team at the Ruhr-University of Bochum for operating the dynamitron tandem accelerator.

References

[1] Street RA, Cahn RW, Davis EA, Ward IM. Hydrogenerated amorphous silicon. Cambridge University Press. Cambridge; 1991.
[2] Gerke S, Becker H-W, Rogalla D, Hahn G, Job R, Terheiden B. Investigation of hydrogen dependent long-time thermal characteristics of PECV-deposited intrinsic amorphous layers of different morphologies. In: Proc 29th EU PVSEC, Amsterdam 2014. p. 9-12.
[3] Dauwe S, Schmidt J, Hezel R. Very low surface recombination velocities on p- and n-type silicon wafers passivated with hydrogenated amorphous silicon films. In: Proc 29th IEEE PVSC, New Orleans 2002. p. 1246-9.
[4] Gerke S, Herguth A, Brinkmann N, Hahn G, Job R. Evaluation of capacitance-voltage spectroscopy by correlation with minority carrier lifetime measurements of PECVD-deposited intrinsic amorphous layers. In: Proc 28th EU PVSEC, Paris 2013. p. 2600-3.
[5] Harbison JP, Williams AJ, Lang DV. Effect of silane dilution on intrinsic stress in glow discharge hydrogenated amorphous silicon films. J Appl Phys 1984;55:946-51.
[6] Pankove JI, Johnson NM, Willardson RK, Beer AC. Hydrogen in semiconductors Vol. 34. Boston: Academic Press; 1991.
[7] Brinkmann NH, Gorgulla A, Bauer A, Skorka D, Micard G, Hahn G, Terheiden B. Influence of electrodes' distance upon properties of intrinsic and doped amorphous silicon films for heterojunction solar cells. Phys Stat Sol A 2014;211(5):1106-12.
[8] Gorgulla A, Brinkmann N, Bauer A, Hahn G, Terheiden B. Influence of the electrodes' distance on the electrical, optical and structural properties of PECV-deposited hydrogenated amorphous silicon films for heterojunction solar cell application. In: Proc 28th EU PVSEC, Paris 2013. p. 744-7.
[9] Ackermann J. Handbuch für die Rasterelektronenmikroskope SUPRA(VP) und ULTRA. Carl Zeiss NTS GmbH, Oberkochen; 2004.
[10] Plagwitz H, Terheiden B, Brendel R. Staebler-Wronski-like formation of defects at the amorphous-silicon-crystalline silicon interface during illumination. J Appl Phys 2008;103:094506.
[11] Danesh P, Pantchev B, Antonova K, Liarokapis E, Schmidt B, Grambole D, Baran J. Hydrogen bonding and structural order in hydrogenated amorphous silicon prepared with hydrogen-diluted silane. J Phys D Appl Phys 2004;37:249-54.
[12] Lanford WA, ^{15}N hydrogen profiling: scientific applications. Nucl Instr and Meth 1978;149(1-3):1-8.
[13] Hanley PR, Cleland MR, Mason CF, Morganstern KH, Thompson CC. The Tandem Dynamitron. IEEE Trans Nuclear Science 1969;16(3):90-4.
[14] Rudolph W, Bauer C, Brankoff K, Grambole D, Grötzschel R, Heiser C, Herrmann F. foils as primary hydrogen standards for nuclear reaction analysis. Nucl Instr and Meth 1986;508-11.
[15] Sinton RA, Cuevas A. Contactless determination of current-voltage characteristics and minority-carrier lifetimes in semiconductors from quasi-steady-state photoconductance data. Appl Phys Lett 1996;69:2510-12.
[16] Kerr MJ, Cuevas A. General parameterization of Auger recombination in crystalline silicon. J Appl Phys 2002;91:2473-80.
[17] Ziegler JF. Handbook of Stopping Cross Sections for Energetic Ions in All Elements. New York: Pergamon Press; 1980.
[18] Fahrner WR, Muehlbauer M, Neitzert HC. Silicon heterojunction solar cells. Material science foundation 31-32. Trans Tech Publications; 2006.
[19] Reinholz U, Weise H-P, Brzezinka K-W, Bremsere W. Zertifizierungsbericht zu BAM-S110, BAM; 2007.
[20] Rizk R, de Mierry P, Ballutaud D, Aucouturier M, Mathiot D. Hydrogen diffusion and passivation processes in p- and n-type crystalline silicon Phys Rev B 1991;44: 6141-51.
[21] Joos S, Herguth A, Hess U, Ebser J, Seren S, Terheiden B, Hahn G. Light induced curing (LIC) of passivation layers deposited on native silicon oxide. En Proc 2012;27:349-54.
[22] Nickel NH et al. Hydrogen in Semiconductors II, Vol. 61. London: Academic Press; 1999.
[23] Staebler DL, Wronski CR. Reversible conductivity changes in discharge-produced amorhous Si. Appl Phys Lett 1977;31:292-4.
[24] Staebler DL, Wronski CR. Optically induced conductivity changes in discharge-produced hydrogenated amorphous silicon. J Appl Phys 1980;51:3262-8.
[25] Stutzmann M, Jackson WB, Tsai CC. Light-induced metastable defects in hydrogenated amorphous silicon: a systematic study. Phys Rev B 1985;32:23-47.